The International Journal of Advanced Manufacturing Technology
https://doi.org/10.1007/s00170-025-16725-y

ORIGINAL ARTICLE

Towards design automation of topology optimized parts: assessment of shape and parametric optimization-based methods

Enrico Dalpadulo[1] · **Luca Guazzini**[1] · **Francesco Leali**[1]

Received: 3 June 2025 / Accepted: 27 September 2025

Abstract
In recent years, Additive Manufacturing has experienced significant growth, yet its full potential is constrained by the lack of clear and easily replicable Design for Additive Manufacturing (DfAM) methodologies. Focusing on the product design stage, the current design approach for topology optimized parts involves an iterative re-design process to identify and reduce stress concentrations based on NURBS modelling, which is hardly replicable and heavily influenced by the designer's experience. This work aims to define two new workflows for DfAM that are easily replicable, highly automated, and based on numerical optimization tools. Leveraging the optimization tools available in 3DExperience integrated CAD platform, after topology optimization, the first workflow involves generating the skeletonization of the resulting geometry and reconstructing it with parametric surfaces, reducing maximum stresses via parametric optimization. The second workflow reconstructs the resulting optimized geometry as a non-parametric B-Rep surface, optimizing maximum stresses through automatic shape optimization. Validation through a case study compares results with the current state-of-the-art approach, evaluating mechanical performance and development lead time, while highlighting designer working time and the pros, cons, and limitations of the proposed methods.

Keywords Design for Additive Manufacturing · Additive Manufacturing · Topology optimization · Shape optimization · Parametric optimization · Design method · Design optimization · 3DExperience

1 Introduction

Additive Manufacturing (AM) is a relatively new material joining process, whereby a product can be directly fabricated from its 3D model [1, 2] (ASTM 2012; ISO 52900). Originating in 1986 with Charles Hull's development of stereolithography, AM initially served for rapid and cost-effective prototyping of aesthetic and functional models. Over time, AM has evolved to encompass a broader spectrum of materials and processes, expanding its application beyond prototyping [3–5] (Gao et al. 2015; Tofail et al. 2017; Ngo et al., 2018). Due to the peculiarity of the layer-by-layer build approach [6] (Pham et al., 1998), AM has multiple advantages over traditional or subtractive manufacturing technologies: It does not require tools; it manages to manufacture complex external shapes without a substantial increase in costs and time [3, 4]. The idea below the outstanding design freedom is that a bi-dimensional shape is easy to create independently from the geometrical complexity of a tridimensional part. Of particular interest is the potential to leverage these characteristics to produce topologically optimized structures, yielding lightweight components and thus attracting interest from sectors such as the aerospace [7–9] (Gu et al., 2020; Zhu et al., 2021; Blakey-Milner et al., 2021) and the automotive [10, 11] (Gray et al., 2020; Sarzynski et al., 2024). Hereafter, topology optimization techniques, their implementation in design strategies, as well as the related limitations, are synthesized.

1.1 Topology optimization

Topology Optimization (TO) is a technique that generates a new design proposal within the concept phase. The aim of TO is to calculate an optimized material distribution within a specified Design Space, under consideration of boundary conditions (i.e., optimization constraints, structural/thermal/fluid boundary conditions and loads). The most popular

✉ Enrico Dalpadulo
enrico.dalpadulo@unimore.it

[1] "Enzo Ferrari" Department of Engineering, University of Modena and Reggio Emilia, Modena, Italy

Published online: 16 October 2025

mathematical method for topology optimization is the Solid Isotropic Material with Penalization method (SIMP), initially proposed by (Bendsoe and Kikuchi, 1988) [12] and (Rozvany et al. 1992) [13]. The SIMP method predicts an optimal material distribution within a given design space, working on finite elements' densities, for given load cases, boundary conditions, manufacturing constraints, and performance requirements.

TO allows for the design of functional and lightweight parts without compromising strength. It can help produce parts with enhanced performance and mechanical properties. This technique optimizes the geometry of an object using mathematical calculations, offering advantages that are not bound by a designer's experience, thus overcoming traditional design limitations. By using TO software, designers can optimize material distribution in specific areas, as the software solves the physical equations for the elements of the discretized domain and removes any unnecessary material from the design. In other words, TO helps create the best possible structure for a given part [14] (Prathyusha et al., 2022). Additive Manufacturing (AM) technologies have enabled the construction of complex and intricate structures, unlocking the full potential of TO [8, 14, 15] (Zhu et al., 2021; Prathyusha et al., 2022; Ibhadode, 2023).

1.2 DfAM of topology optimized parts

Many designers encounter significant obstacles in fully utilizing the unique advantages offered by AM. To overcome these obstacles, it is essential to develop specialized design methodologies that align with the distinct capabilities of AM technologies. These methodologies should not only enhance the manufacturability of AM-produced products but also optimize their functional performance by leveraging the specific strengths of AM techniques. The concept of Design for Additive Manufacturing (DfAM) has emerged as a critical approach to address these needs. DfAM is defined as a set of design strategies that optimize functional performance and other key product lifecycle considerations — such as manufacturability, reliability, and cost — within the constraints and possibilities of AM technologies [16] (Tang & Zhao, 2016). The idea of DfAM first gained attention around 2009, when Bourell advocated for the creation of new design methods tailored to AM, drawing inspiration from established principles like Design for Manufacturing (DfM) and Design for Assembly (DfA) [17] (Bourell et al., 2009). Since then, the understanding of DfAM has evolved, with various definitions and frameworks being proposed. Recent efforts have focused on classifying DfAM approaches, often using systematic design principles like VDI 2221 [18] (Kumke et al., 2016) or dividing the design process into sequential design and manufacturing stages [19] (Pradel et al., 2018). According to the latest approaches, DfAM should be structured along three main phases: task design (system design level — or suitability exploration), product design, and process design [20, 21] (Wiberg et al., 2019; Vaneker et al., 2020) (Fig. 1). These efforts aim to provide a robust framework for designers to fully leverage the potential of AM in developing innovative and efficient products.

The current and consolidated workflow for the design of topology-optimized parts, as also depicted in the latest reviews [14, 15, 22] (Sotomayor, 2021; Prathyusha, 2022; Ibhadode, 2023), is now synthesized. The workflow begins with the initial 3D CAD model. This model represents the original, non-optimized design, which is subjected to structural analysis to evaluate its physical behavior (e.g., stress distribution) under loading conditions. Based on this analysis, areas of the part that experience minimal stress are identified as candidates for material removal. The next stage, known as Pre-Processing or Geometry Preparation, involves defining the design space, or rather the volume within which TO will occur. This includes setting up both the Design Space, where material distribution is flexible, and the Non-Design Space, which defines regions that must remain intact for functional reasons. Once the geometry is prepared, the Optimization Setting follows, where the 3D model is discretized into a finite element mesh, and appropriate loads, restraints, and optimization targets are applied. The TO process then iteratively removes material to achieve a lightweight and structurally efficient design. As schematized in Fig. 2, the resulting optimized geometry undergoes Post-Processing, including re-design (Geometry Interpretation), which is then iteratively refined to meet specific functional, aesthetic, or manufacturability requirements, such as those dictated by DfAM principles. This may involve validating the optimized design through numerical (e.g., Finite Element Analysis (FEA)) or analytical methods, and if necessary, re-running the optimization with adjusted parameters. Such workflows have been widely adopted in various DfAM studies, from early aeronautical [23] (Gebisa Lemu, 2017), aerospace [24] (Orme et al., 2018), and automotive [25, 26] (Reddy, 2016; Walton, 2017) applications. Without any substantial improvements, it has also been used for more recent and complex designs, ranging from structural parts (e.g., steering uprights [27] (Mantovani et al., 2021), suspension rockers, or brake pedals [28] (Barbieri et al., 2022)) and functionally optimized parts (e.g., brake calipers [29, 30] (Ugemuge et al., 2020; Tyflopoulos et al., 2021)) to various other applications [14, 15] (Prathyusha, 2022; Ibhadode et al., 2023).

1.3 Research gap

1.3.1 Context

Throughout the literature, there is a recurring theme that the realization of AM's full potential heavily depends on

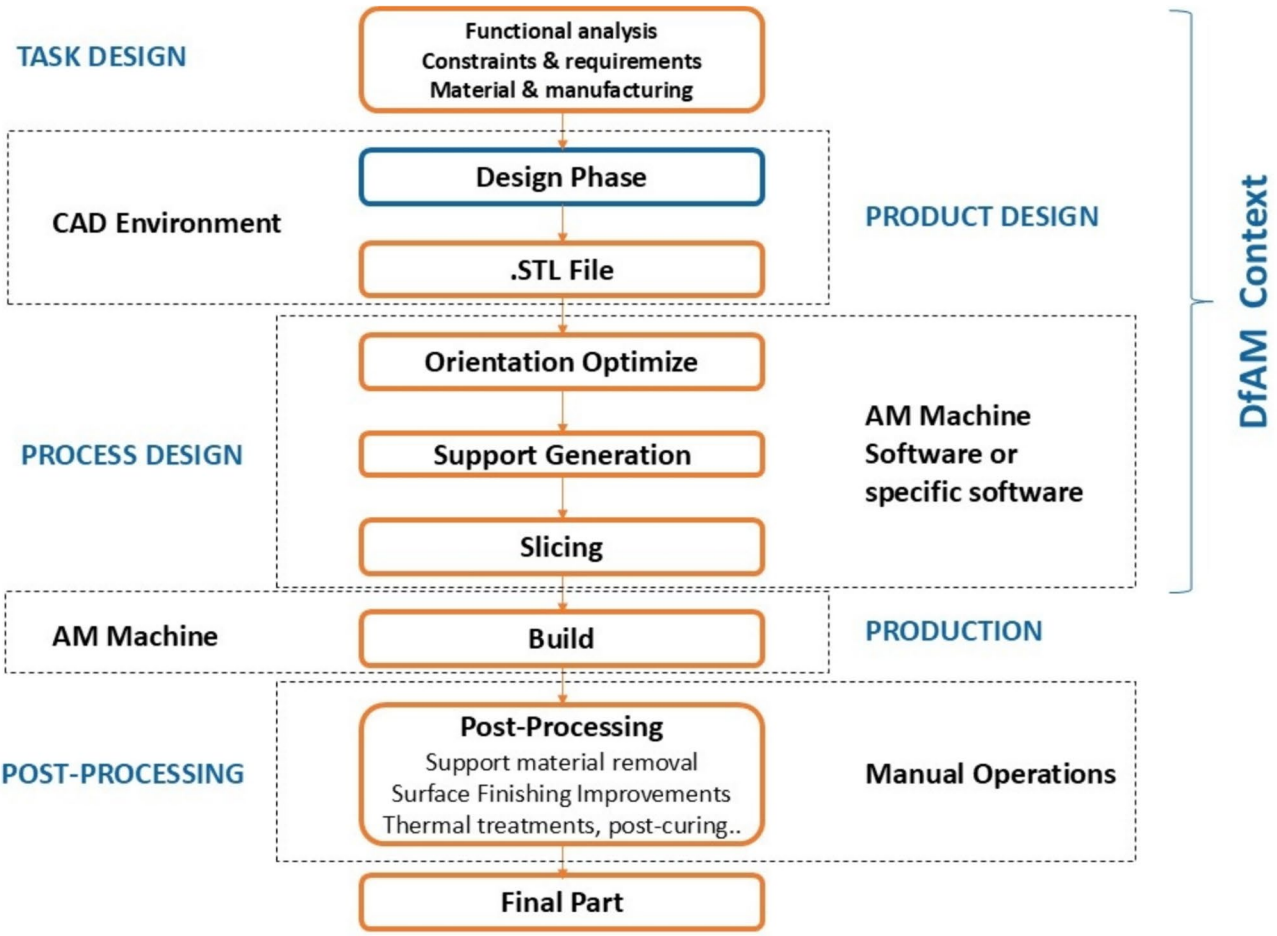

Fig. 1 Schematic of the additive manufacturing process, from task design to finished part

the development and adoption of robust DfAM methodologies. The deficiency in a comprehensive understanding and implementation of DfAM impedes Additive Manufacturing's market penetration and restricts its utilization by designers [16, 19, 31–34]. The lack of structured knowledge of DfAM approaches has been identified as one of the barriers holding back further adoption of AM in the industry [21] (Vaneker et al., 2020). The studies conclude that, to optimize the workflows, not only systematic knowledge but also increased integration and automation are needed [20, 21] (Wiberg et al., 2019; Vaneker et al., 2020). This paper develops and validates practical approaches to streamline the design of topology-optimized parts.

1.3.2 Issues

This work focuses on the Product Design phase (Fig. 2), for which attempts to improve the described workflow through systematic approaches have been proposed [35, 36] (Dalpadulo et al., 2021, 2024) and have also been adopted in more recent works, such as by [37] (Holub et al., 2023). In particular, our focus is on the TO post-processing, highlighted by the dotted line in Fig. 2. In fact, a critical step in the design based on topology optimization is the Geometry Interpretation and subsequent refinement. Translating topological results into tangible models often necessitates manual intervention, such as reconstruction using Non-Uniform Rational B-Splines (NURBs). Therefore, following topology optimization, an iterative re-design process based on Geometry Interpretation [22, 38] (Sotomayor, 2021; Fuchs, 2022) and a manual redesign phase occurs to further reduce stress concentrations, a process which is repeated until the desired result is achieved. This process is difficult to replicate and is heavily influenced by the designer's experience.

1.3.3 Hypotheses and related works

To address these issues, we explore the utilization of numerical optimization techniques to automatically refine topology-optimized designs, aiming to produce ready-to-print geometries with minimal user intervention. In the literature, researchers aim to streamline the design of 'ready-to-print'

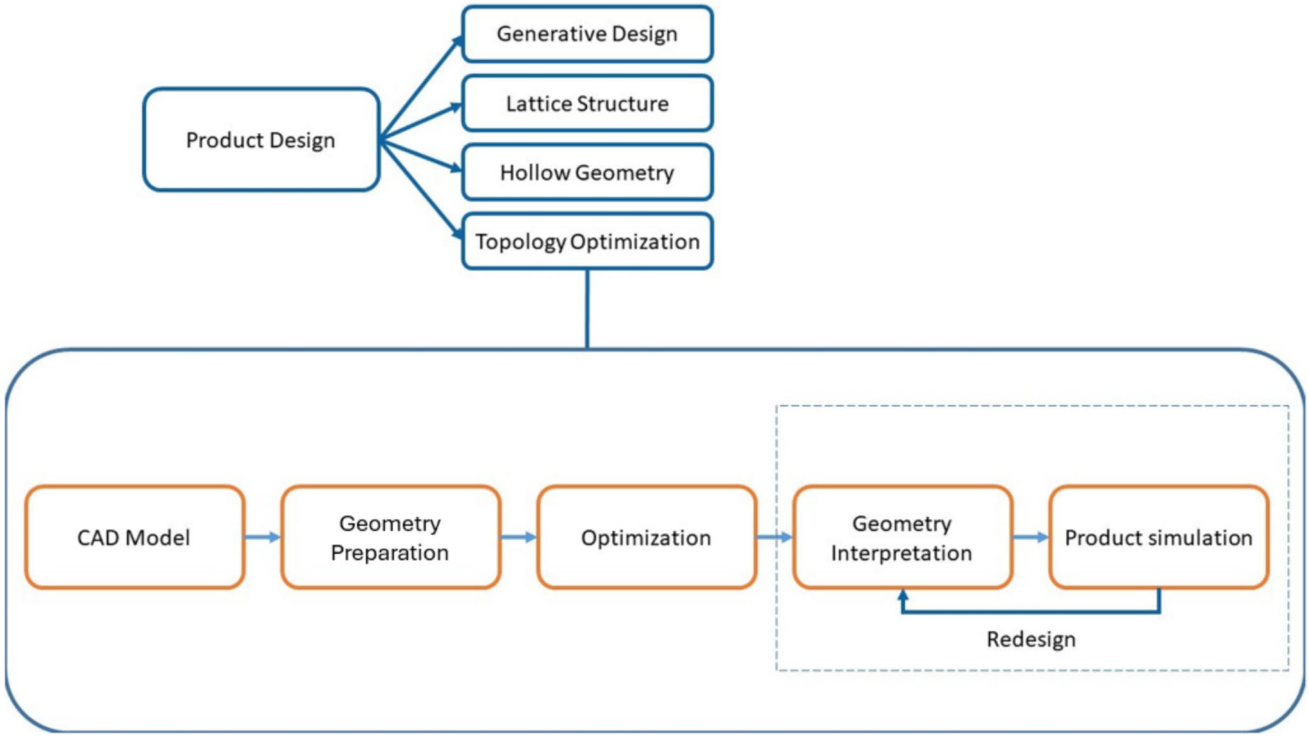

Fig. 2 Schematic of the Product Design phase based on Topology Optimization workflow

parts through various design approaches. Xiao et al. first assessed the possibility of performing a redesign followed by numerical shape optimization [39] (Xiao et al., 2017). This approach improves post-processing efficiency, but manual geometry interpretation is still required. Tyflopoulos et al. analyzed and compared TO with a numerical parametric optimization technique, concluding that specific methods to properly combine these tools should be developed [40] (Tyflopoulos and Steinert, 2020). Other approaches are based on the skeletonization of the TO result, followed by specific CAD boundary-representation (B-rep) generation and subsequent refinement steps. Biedermann et al. developed an approach based on skeletonization and loft-based geometry creation for the specific design of hydraulic manifolds [41] (Biedermann et al., 2021). A similar approach was used by Amroune et al., who developed an effective redesign strategy based on skeletonization and loft-based reconstruction for different beam-like structural parts [42] (Amroune et al., 2022). Mayer et al. developed an almost fully automated approach for the reconstruction of non-beam-like geometries and B-rep generation [43] (Mayer et al., 2022). Nevertheless, further design refinement (e.g., by FEA) remains challenging. In fact, besides improving and demonstrating the method with many possible geometries, they concluded that results could be enhanced through a numerical parametric optimization task [44] (Mayer et al., 2023). Finally, Sedlacek et al. utilized convergent-model generation instead of remodelling the TO result [45] (Sedlacek et al., 2023), which proves to be an efficient post-processing stage; however, it still doesn't eliminate the possible need for iterations between TO and FEA.

1.4 Research goal

The AM process can be divided into several stages (Fig. 1). This work focuses on the Product Design phase, which constitutes the core of the DfAM workflow. Among the available design strategies—such as generative design, lattice structures, hollow geometries, and topology optimization—this research focuses on TO. The approaches proposed in this study retain the early stages of the traditional TO workflow but introduce numerical methods—specifically Parametric Optimization and Shape Optimization —to reduce manual intervention in the post-processing phase. The research operational perimeter is delimited by the dotted line in Fig. 2. The goal is to automate and enhance the refinement of TO results, improving design efficiency and reliability. Once the optimized geometry is finalized, the subsequent AM workflow steps can be performed using conventional practices (Fig. 1). The methods introduced are technology-independent, ensuring applicability across different AM processes. In this research, metal Laser Powder Bed Fusion (L-PBF) is adopted as a representative case study.

1.4.1 Paper structure

The paper is organized as follows: Sect. 2 analyzes the selected numerical techniques and related tools and describes the investigation approach; Sect. 3 develops and introduces the novel design methods, while Sect. 4 implements the proposed workflows in the design of a topology-optimized automotive case. Section 5 compares the novel design methods with respect to the workflow consolidated in the state of the art. Finally, Sect. 6 presents the concluding remarks.

2 Material and methods

To reduce the need for iterative design loops between modelling and simulation stages, two numerical optimization techniques are selected as the object of investigation. In fact, parametric and shape optimization tools may be adopted to achieve 'ready to print' parts while minimizing the designer's intervention. Hereafter, the fundamentals of the techniques are introduced, as well as the related software tools and their preliminary study is synthesized.

2.1 Theory

The first step in understanding the operation of optimization tools is to focus on the underlying mathematical principles that guide their functionality.

Localized stress concentrations can reduce the lifespan of parts, leading to sudden failures under static, dynamic, or fatigue loads. Therefore, it is crucial to analyze stress concentrations in the independent segments of the product. Reducing local stresses and further mass can be achieved through optimization techniques such as parametric or shape optimization.

2.1.1 Parametric optimization

Parametric optimization adjusts input parameters to drive the output (objective) in a desired direction, such as minimizing or maximizing mass. Design constraints, like peak stress, can be set within a prescribed range. The process iterates based on previous results, ending after a set number of iterations or time limit. Objectives and design constraints include parameters like mass and volume, while design parameters cover geometry and analysis variables. Unlike single-objective non-parametric optimization, which requires separate optimizations for each parameter value, parametric optimization provides optimal solutions as functions of parameters within feasible ranges. Multiparametric optimization addresses problems with unknown parameters during optimization.

Below is the general formulation of a parametric optimization problem:

$$Z(t) = \min_{x,t} f(x,t) \tag{1}$$

Subject to:

$$g_i(x,t) \le 0, \quad i = 1,2,\dots,m \tag{2}$$

$$h_j(x,t) = 0, \quad j = 1,2,\dots,n \tag{3}$$

$$x \in X \subset \mathbb{R}^p \tag{4}$$

$$t \in x\Theta \subset \mathbb{R}^q \tag{5}$$

$$x_{lb} \le x \le x_{ub} \tag{6}$$

where $\boldsymbol{x}$ is a vector of design variables, $\mathbf{t}$ is a vector of parameters, $\boldsymbol{X}$ is a set of feasible designs, Θ is a set of parameters, Rp and Rq are vector spaces of dimensions p and q respectively. Additionally, $f(\boldsymbol{x}, \boldsymbol{t})$ is a parametric objective function, $gi(\boldsymbol{x}, \boldsymbol{t})$ are parametric inequality constraints and $hj(\boldsymbol{x}, \boldsymbol{t})$ are parametric equality constraints, and m and n are the number of inequality and equality constraints, respectively. Finally, $\boldsymbol{xlb}$ and $\boldsymbol{xub}$ are lower and upper bounds, respectively, for the design variables [46] (Ravichandran et al., 2019).

2.1.2 Shape optimization

The finite element-based shape optimization problem can be defined as follows:

$$\min_{d} f(x, u(x)) \tag{7}$$

Subject to:

$$g_j(x, u(x)) \le 0 \qquad j = 1,\dots,l \tag{8}$$

$$K(x)u(x) = f(x) \tag{9}$$

$$\boldsymbol{x} = \tilde{\mathbf{x}}(\boldsymbol{d}) \tag{10}$$

where f denotes the objective function to minimize; gj denotes the constraint functions; $\boldsymbol{d} \in \boldsymbol{Rm}$ denotes the m-dimensional design variable vector; $\boldsymbol{x} \in \boldsymbol{Rn}$ denotes the n-dimensional finite element node coordinate vector; $\boldsymbol{u}$ denotes the nodal displacement vector; $\boldsymbol{K}$ denotes the global stiffness matrix; $\boldsymbol{f}$ denotes the nodal force vector; and $\tilde{\boldsymbol{x}} : \boldsymbol{Rm} \rightarrow \boldsymbol{Rn}$ denotes the mapping from $\boldsymbol{d}$ to $\boldsymbol{x}$.

Shape optimization uses a filter on objective function sensitivities, constraint sensitivities, and design variables to achieve smooth results. The optimization algorithm

calculates a displacement vector for each design node, which represents the direction of optimization, corresponding to the outer surface unit normal. These vectors are updated in each design cycle based on changes in structure shape, constraints, and mesh quality. This method is based on the independent node movement approach so that.

$$\boldsymbol{x} = \tilde{\mathbf{x}}(\boldsymbol{d}) \ = \boldsymbol{d} \tag{11}$$

According to this approach the filtered sensitivity,

$$\frac{\partial f}{\partial d} = \frac{\partial f}{\partial x} \tag{12}$$

are processed by the optimizer to compute the search direction s, which is used to update the design,

$$d^{l+1} = d^{l} + \alpha s \tag{13}$$

where $\alpha > 0$ is the step length. However, before proceeding with the one-dimensional search, s is smoothed. Akin to the natural design variable method, the search direction s serves as the load in a fictitious shape change analysis of the current design. The resulting fictitious displacement $\tilde{\boldsymbol{u}}$ induced by this load s is returned to the optimizer in lieu of the original search direction s so that.

$$d^{l+1} = d^{l} + a\tilde{u}. \tag{14}$$

$\boldsymbol{dI}+1=\boldsymbol{dI}+\alpha\tilde{\boldsymbol{u}}$. In this way the design update is smooth [47] (Le et al., 2011).

2.2 Tools

Central to this investigation is the use of Integrated CAD Platforms, which eliminate the need for repeated exporting and importing of data between software tools, along with the selection of commercial software to facilitate implementations and practical applications. In most cases, various specialized software tools are employed to carry out different tasks within DfAM workflows, which can lead to workflow issues, particularly concerning data management and exchange [22, 38, 48] (Reiher, 2017; Sotomayor, 2021; Fuchs, 2022). Integrated CAD platforms, on the other hand, offer a solution to these workflow issues by maintaining parametricity and associativity between different CAD-based environments. A previous work assessed the use of integrated CAD platforms to support conventional DfAM methodologies [35] (Dalpadulo, 2022). The tools adopted in this investigation are those provided by Dassault Systèmes' integrated CAD platform, 3DExperience. Of particular relevance to this study are the Parametric Optimization and Shape Optimization tools embedded within the Structural Generative Design application. These tools are subject to investigation to assess their potential integration into novel design workflows following Topology Optimization. The intent is to replace the manual redesign phase with automated approaches. We remark that developing design methods integrating modelling, simulation and optimization tasks within a unified CAD/CAE environment, which are based on leveraging commercial software tools, would allow effective implementation in industrial applications.

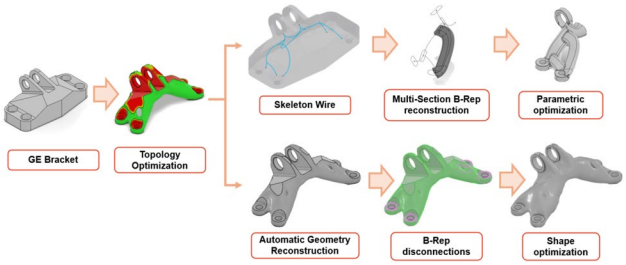

Fig. 3 Schematic of the two proposed workflows for product design based on topology optimization

2.3 Investigation approach

To achieve the research objectives, the Parametric Optimization and Shape Optimization tools are examined. Their advantages, disadvantages, constraints, limitations, and optimal parameter settings are assessed.

To conduct this analysis, two significant geometries representing typical structures found in topology-optimized designs are identified and represented through a parametric model (Sect. 3.1). A preliminary study was based on (i) Finite Element Analyses (FEAs) on the optimized components, performing also mesh sensitivity analyses to define settings balancing effectiveness, and (ii) the assessment of structural Key Performance Indicators (KPIs) (sections. 3.2, 3.3). Also, the functionality of the shape optimization tool on a non-parametric B-Rep surface automatically generated by TO was assessed, as well as the feasibility of generating a skeletonized version of the TO and systematically reconstructing it using parametric surfaces was explored. The preliminary study can be found in [49] (Dalpadulo, 2025) and the results are synthesized in Sects. 3.13.3–3.3. Based on these initial findings, two novel workflows will be defined.

Basically, the design workflows, which are developed, described, and implemented in Sects. 4–5, can be schematically represented from a conceptual point of view, as shown in (Fig. 3).

Once the workflows are delineated, a case study is selected to validate them. The results obtained using these new approaches are compared with those achieved through the current state-of-the-art workflow in DfAM (Sect. 1.2). Several Key Performance Indicators (KPIs) are selected to support an accurate assessment. For assessing mechanical performance, the safety factor, maximum displacement, and

mass are evaluated. To assess the extent to which the process depends on the designer's input versus being executed by numerical optimization tools, the total design time and the time spent by the designer are considered. Finally, conclusions are drawn, discussing the positive results, highlighting limitations, and exploring the potential for future developments.

3 Novel design methods

To explore the tools of shape optimization and parametric optimization, it is necessary to select a simple but representative geometry to obtain meaningful results.

3.1 Representative geometries for testing

Since both optimizations are integrated into the design workflow following a topology optimization step (Fig. 3), it is logical to select a geometry for testing that reflects the characteristics of a topology-optimized structure. Upon examining such structures, it becomes evident that they predominantly consist of branched tubular geometries, which either connect to other branches or interface with non-design regions, such as holes, bolt attachments, or supports. Consequently, two representative test geometries are modelled: the first simulates the intersection of two distinct branches (referred to as a Node-Arc Topology — A, Fig. 4a), while the second represents the connection between a branch and a non-design region (referred to as a Node-to-Polygon Topology — B, Fig. 4c). These two configurations capture the recurring morphological features observed in topology-optimized structures. Figure 4b illustrates an automotive component alongside the simplified geometries abstracted from the topology-optimized structure's morphology.

The models (Fig. 4a, c) were tested under two load cases —compression and tension—with 1000 N forces applied parallel to the vertical branch axis to simulate real-world mechanical stress conditions (Fig. 5a). A was constrained at the vertical faces, while B included a virtual bolt constraint to restrict radial degrees of freedom at the connection point. A FEA approach was used to measure stress distribution, displacement, and mass efficiency before and after optimization. Mass preservation and maximum stress reduction were therefore explored. Additional details can be found in [49] (Dalpadulo, 2025).

3.2 Parametric optimization study

The study on parametric optimization focused on refining topology-optimized structures by adjusting geometric parameters while maintaining the overall topology. Key parameters, such as the branch diameters and the fillet radius between them, were selected as design variables for the optimizer. Each parameter was allowed to vary within ± 20% of its nominal value, with an iterative step equal to 10% of this range, while respecting predefined bounds. The objective of the optimization was to minimize stress concentrations while preserving the overall mass of the component. Figure 5c and e shows examples of geometries obtained through parametric optimization that achieve stress reduction while maintaining constant mass.

A mesh sensitivity study was performed to evaluate the influence of mesh size during the parametric optimization phase. Quadratic meshes with element sizes of 1.582 mm, 3.164 mm, and 6.328 mm were tested, along with a linear mesh of 3.164 mm. These varying resolutions produced distinct optimized geometries. To isolate the effect of mesh resolution, all resulting geometries were analyzed using the same quadratic mesh with an element size of 1.582 mm. The findings indicate that employing a finer quadratic mesh during optimization leads to a more accurate and effective process. Lower maximum stress values in both models A (Fig. 5e) and B (Fig. 5c) were achieved with a 20% stress reduction compared to the initial design. Additionally, the use of partitions around constrained areas, such as bolt holes, improved the optimization process by providing a more uniform stress distribution. More, two additional steps are needed for the implementation, i.e. (i) the skeleton wireframe manipulation (e.g., parametric cross-sections creation) and (ii) the multi-section B-rep construction. Despite its advantages in automated design exploration, parametric optimization was found to be sensitive to initial conditions and required careful parameter selection for effective results.

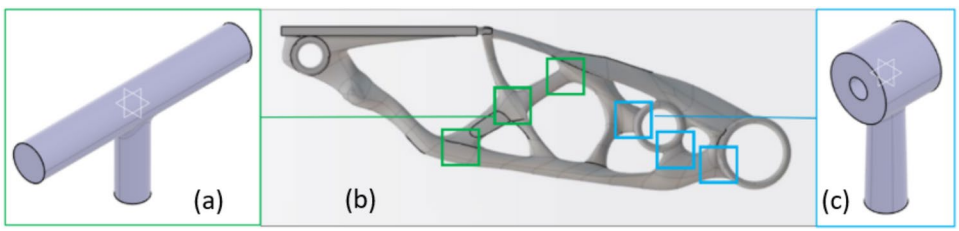

Fig. 4 Topology-optimized structure (**b**) and simplified representative geometries: Node-Arc Topology.— A (**a**) and Node-to-Polygon Topology — B (**c**)

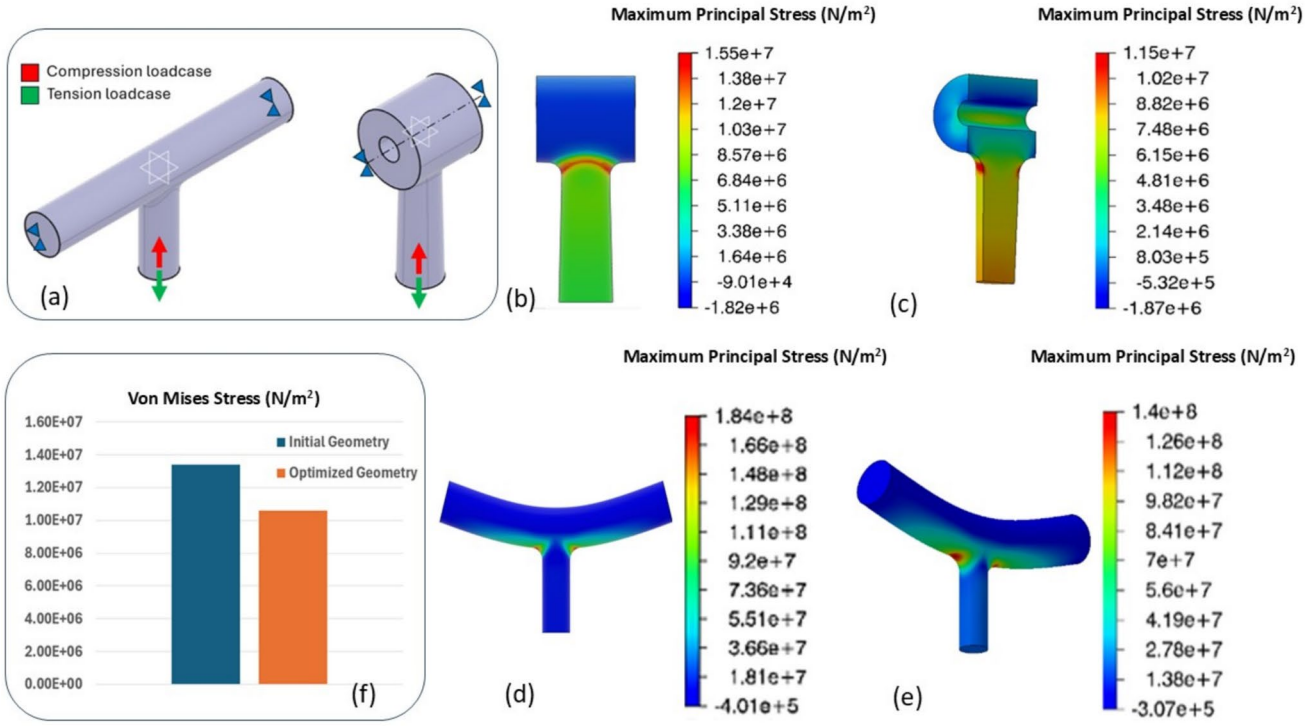

Fig. 5 Load cases of the test geometries (**a**); Maximum Principal Stress analysis under the tensile load case for the initial geometries of Node-Arc Topology — A (**d**) and Node-to-Polygon Topology — B (**b**); stress analysis for the geometries obtained after parametric optimization for A (**e**) and B ({g}_{j}\left(x,u\left(x\right)\right)\le 0 j=1,\dots,l); Von Mises stress comparison between the initial and optimized geometries for B (**f**)

3.3 Shape optimization study

The shape optimization study explored modifying structural boundaries to improve performance while preserving topology. Unlike parametric optimization, which adjusts parameters within fixed geometry, shape optimization allows free-form deformation of the structure's surface to minimize stress concentrations and enhance mechanical properties.

The study then compared both manually redesigned (NURBS) and automatically generated (B-Rep) and surfaces (Fig. 6a). A mesh sensitivity analysis was also carried out for the study of the shape optimization tool, following the same procedure described in Sect. 3.1. However, unlike parametric optimization, where finer quadratic meshes consistently improved the results, shape optimization proved to be less sensitive to mesh size variations. No direct correlation was observed between reducing the mesh element size during the optimization phase and a decrease in the maximum stress of the optimized geometries. Figure 6c and e depicts examples of stress reduction while maintaining constant mass provided by shape optimization of a NURBS model. The results showed that automatic B-Rep models derived directly from topology optimization could be refined without manual intervention, but NURBS-based surfaces performed better in reducing stress (Fig. 6f). Optimization of the models yields excellent results with maximum stress reduced by 20%—60%. While shape optimization provided greater flexibility in improving performance, it required pre-processing steps, such as geometry disconnection and reconstruction, which added complexity.

3.4 Workflows definition

Both techniques demonstrated significant stress reductions, but shape optimization generally outperformed parametric optimization in terms of maximum stress reduction—63% improvement in some cases. However, parametric optimization offered a structured and repeatable workflow, making it more accessible for direct CAD integration. Based on the results obtained from the preliminary study [49] (Dalpadulo, 2025), it is now feasible to proceed with defining two innovative workflows for additive manufacturing design, leveraging the numerical tools described earlier. After TO, these approaches (conceptualized in Sect. 2.3), aim to achieve a highly automated design process that is easily repeatable and less reliant on the skills and expertise of the designer.

- **Skeleton-Based Parametric Optimization (SPO) Method.** It is based on generating the skeleton of the topologically optimized geometry. Subsequently, the

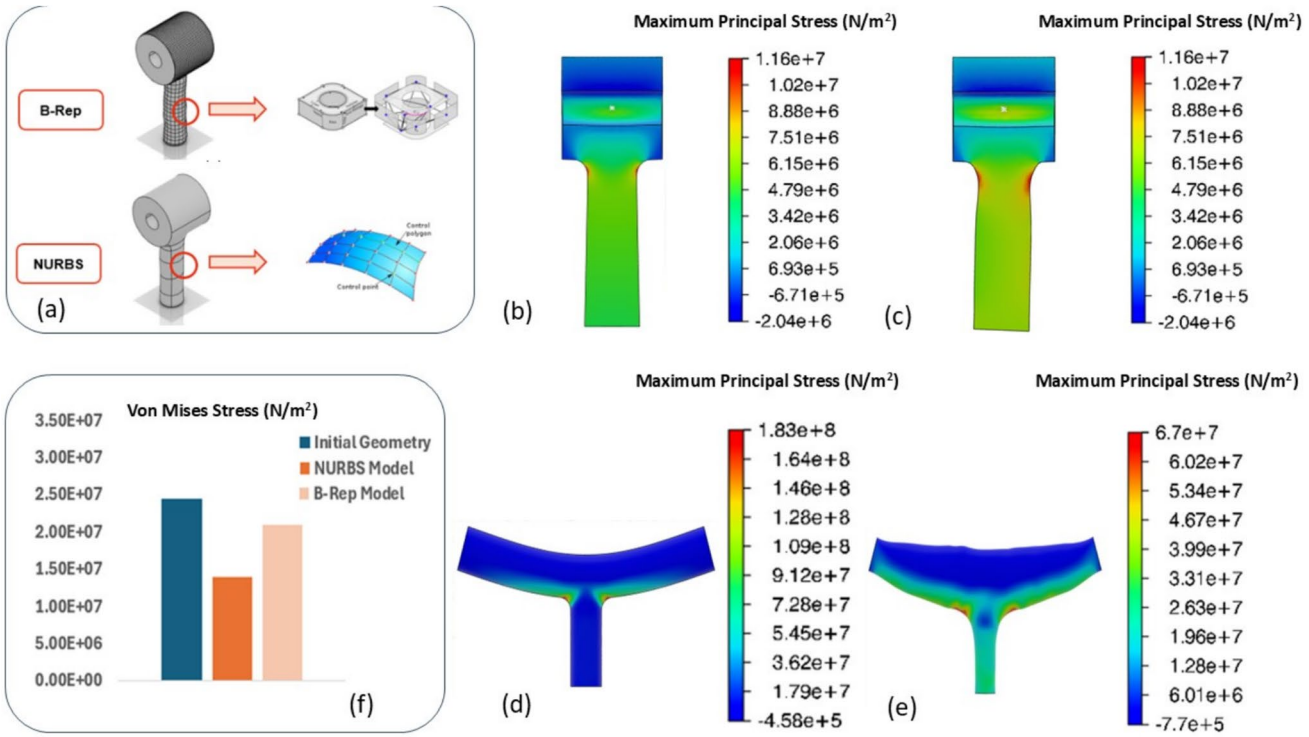

Fig. 6 B-rep and NURBS models (**a**); Maximum Principal Stress analysis under the tensile load case for the initial geometries of Node-Arc Topology — A (**d**) and Node-to-Polygon Topology — B (**b**); stress analysis for the geometries obtained after shape optimization for A (**e**) and B (**c**); Von Mises stress comparison between the initial and optimized geometries for B, considering both a redesign using NURBS surfaces and an optimization performed directly on the B-Rep surface (**f**)

geometry is reconstructed using parametric surfaces and subjected to parametric optimization to reduce maximum stresses.

- **Auto B-Rep Shape Optimization (ABSO) Method.** It is based on the use of the shape optimization tool to directly optimize the non-parametric surface generated as a result of topology optimization.

Both methods will be illustrated in the next section through a case study.

4 Results: validation

To validate the effectiveness of the innovative design workflows, Skeleton-Based Parametric Optimization (SPO) and Auto B-Rep Shape Optimization (ABSO), the brake pedal installed on the Formula Student car of the MoRe Modena Racing (MMR) Driverless team is selected for analysis (Fig. 7a). The results obtained will then be compared with those achieved using the current state-of-the-art (SOA) method.

As a critical component of the vehicle's braking system, the brake pedal is essential for controlling speed and maintaining stability during braking maneuvers. It enables the driver to modulate braking force through foot pressure while also accommodating autonomous braking in driverless scenarios. To comply with regulations, the pedal must withstand a load of at least 2000 N.

Accordingly, two load cases are analyzed, each applying a force of 2000 N. The first case represents braking initiated by the driver's foot (Fx(A), Fig. 7b), while the second considers the intervention of the autonomous braking system (Fx(B), Fig. 7b).

The initial steps of model preparation and topology optimization are identical for both the innovative workflows proposed in this paper (SPO, ABSO) and the state-of-the-art (SOA) approach. These steps, which are detailed below, can be performed with a conventional SIMP-based TO, and ensure a consistent starting point before the workflows diverge.

4.1 Model preparation

An assembly analysis is performed to derive the largest possible Design Space (Fig. 7c), allowing greater flexibility for the optimization tool, while simultaneously ensuring the proper assembly and functionality of the component.

Once the Design Space is modelled, it is necessary to proceed with its partitioning before conducting Topology

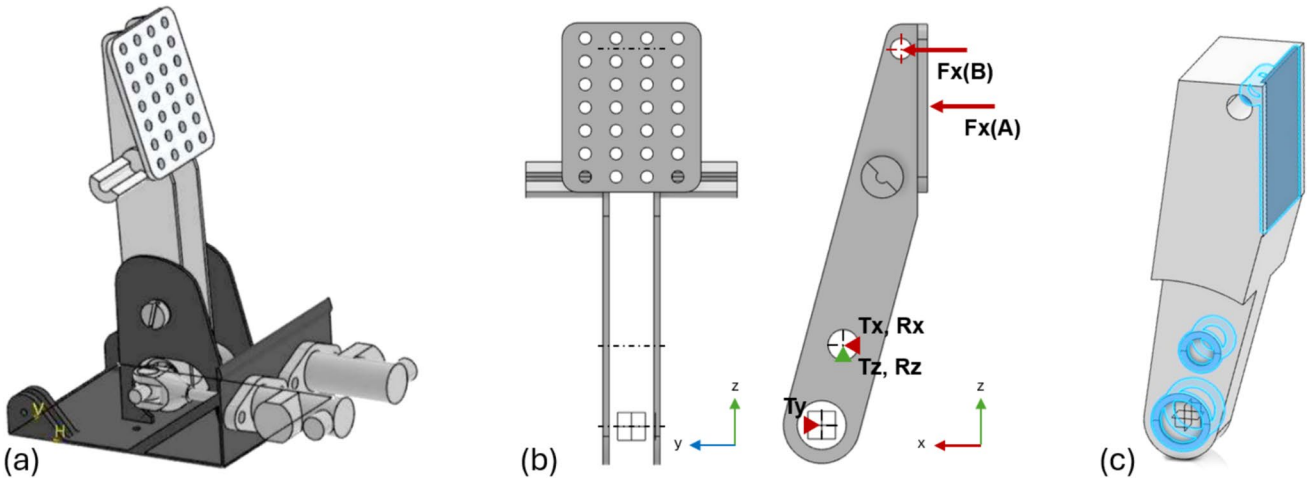

Fig. 7 Brake pedal of the MMR Driverless car (**a**), load cases (**b**), and design space (**c**)

Optimization. Partitioning defines the areas that should not be altered during the optimization process. In this case, the zones to be preserved include the hole through which the connection between the structure and the brake pedal occurs, the hole facilitating the connection between the pedal and the braking system, the hole connected to the autonomous braking system, and the pad enabling the drivers to apply pressure with its foot to brake (Fig. 7c).

The selection of a suitable material is now underway. It is essential to opt for a material with excellent mechanical properties while also enabling the creation of a lightweight component compatible with the production technology. Therefore, the choice falls on the aluminium alloy AlSi10Mg, available in powder form for manufacturing parts using the Laser Powder Bed Fusion additive manufacturing technology.

The goal of this redesign is to enhance the component's mechanical performance while reducing its weight. The results of the redesigned component are compared with those from the state-of-the-art (SOA) approach. To ensure an objective evaluation, several key performance indicators (KPIs) are selected, including the safety coefficient, maximum displacement (mm), and mass (kg), providing a comprehensive assessment of mechanical performance.

Furthermore, to gauge the impact of human intervention versus numerical optimization tools, the total design time [min] and the designer's working time [min] are considered (Fig. 8).

4.2 Topology optimization

Proceeding with Topological Optimization, the previously partitioned design space (Fig. 7c) is selected as the optimization region. The two load cases (Fig. 7b) are considered for the analysis. A preliminary analysis of the design space is conducted using a 2.141 mm mesh size, to identify areas where material should be added or removed.

Next, the Topology Optimization tool is configured. A mesh size of 3.3 mm is chosen for the optimization case, with the objective of maximizing stiffness for a given mass, commonly employed with a SIMP-based method. Assuming a weight reduction of approximately 20 percent compared to the initial component weight of 0.497 kg, an absolute mass target of 0.280 kg is set to allow greater flexibility in fine-tuning the final shape by adjusting the cutting value. To ensure symmetry, a geometric constraint is applied. Additionally, a Minimum Thickness constraint of 10 mm, which is equivalent to three times the mesh size, is imposed.

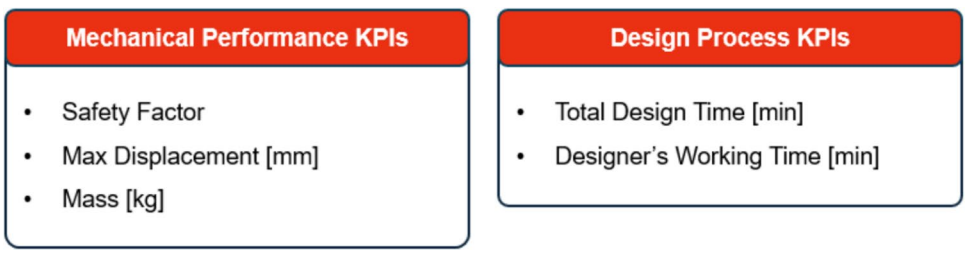

Fig. 8 Key Performance Indicators (KPIs) for evaluating the redesigned component

4.3 SPO method redesign

Once the common steps across the different methods are completed, the first redesign is performed using the SPO workflow (Fig. 9).

4.3.1 Skeleton wire generation

Once the topological optimization process is completed, the Concept Generation is performed, selecting the Skeleton Wire as the output. The Cutting Value selected is set to 57 to achieve a mass similar to the target mass and to maintain consistency with the other methods. The obtained result is then modified with surface design tools to facilitate the surface reconstruction process. Subsequently, spline adjustments are made to ensure that intersections between different wires occur between no more than two of them. Additionally, new spline points are placed at the center of non-design zones to ensure seamless integration with the surfaces to be reconstructed. It is crucial during this process to avoid alterations that may significantly deviate the skeleton from its topologically optimized form.

4.3.2 Surface reconstruction

Orthogonal planes are added along the splines passing through the extremal points. Elongated holes with dimensions comparable to the structures obtained from topological optimization are then sketched on these planes. Next, Non-Design zones are initially modelled using surfaces. Subsequently, Multi-section surfaces are generated, with elongated holes serving as sections and splines as guides. This results in a distinct surface for each branch. Trim operations are subsequently executed between the different surfaces until a unified closed surface is achieved. Fillets are introduced at intersections, both between different branches and between branches and non-design zones. At the end of this process, a single parametric surface representing the topologically optimized geometry is obtained.

4.3.3 Solid body transformation

After achieving a single closed surface, the subsequent step involves constructing a solid body with identical geometry. This is accomplished by executing a split operation between the surface and a solid cubic body, sized to entirely enclose the previously obtained surface. Once the solid body is obtained, partitions around the holes are extracted with a 3 mm offset. The geometry is manually adjusted to ensure compliance with the spatial constraints set by the Design Space. This manual modification guarantees the functionality and assembly of the component.

4.3.4 Parameters selection

The parameters to be adjusted for optimization are carefully selected. For each section, two parameters are chosen: the horizontal and vertical dimensions. Additionally, the fillet

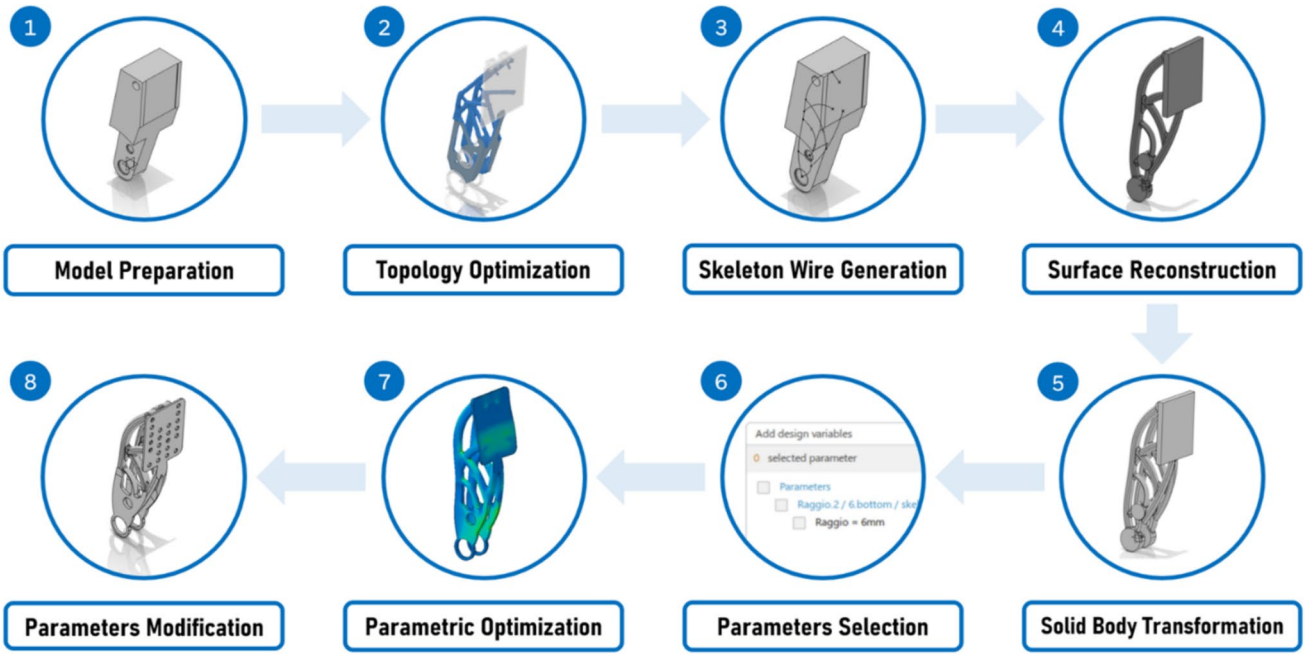

Fig. 9 Schematic of the redesign process using the SPO workflow

radii are included as parameters for optimization. Meaningful names are assigned to each parameter to facilitate their identification. Each parameter is assigned a variation range of ± 30% relative to its initial value, with iteration steps set to 1/10 of this interval. In total, 32 parameters are selected for optimization.

4.3.5 Parametric optimization

The Parametric Optimization tool is configured to achieve the objective of Minimizing Maximum Stress. Furthermore, a constraint is applied to the mass, defining an acceptable range spanning from 70 to 80% of the weight of the non-optimized component. The selected mesh size for optimization is 2.141 mm. Sampling is set to Guided, with the maximum possible number of calculation points defined as 32. In 9 out of the 32 calculation points, there is a failure in reconstructing the geometry or the mass constraint is violated. The optimal result is found at calculation point number 29.

4.3.6 Manual parameter modification

After completing the optimization process and obtaining the optimal parameter values, manual modification of these parameters on the model is required. With meaningful names assigned, this operation becomes more straightforward. Upon completing the parameter adjustments, the final optimized geometry is achieved.

4.4 ABSO method redesign

Similarly, the redesign is conducted following the ABSO workflow (Fig. 10).

4.4.1 Concept generation

Once the topological optimization process is completed, the Concept Generation proceeds using the Subdivision Surface method. The Cutting Value selected is set to 57 to achieve a mass similar to the target mass. In this case, the generated geometry has a mass of 0.446 kg. The generated geometry is analyzed using a mesh size of 2.141 mm.

4.4.2 Geometry disconnection

Prior to initiating the shape optimization, it is essential to isolate the portion of the geometry intended for optimization by disconnecting it. This disconnection is carried out on the topologically optimized geometry, specifically excluding the brake pad from the optimization process.

4.4.3 Shape Optimization

The Shape Optimization proceeds by selecting the recently disconnected geometry for optimization. Optimization is set with the objective to minimize maximum stress while keeping the mass constant. A mesh size automatically

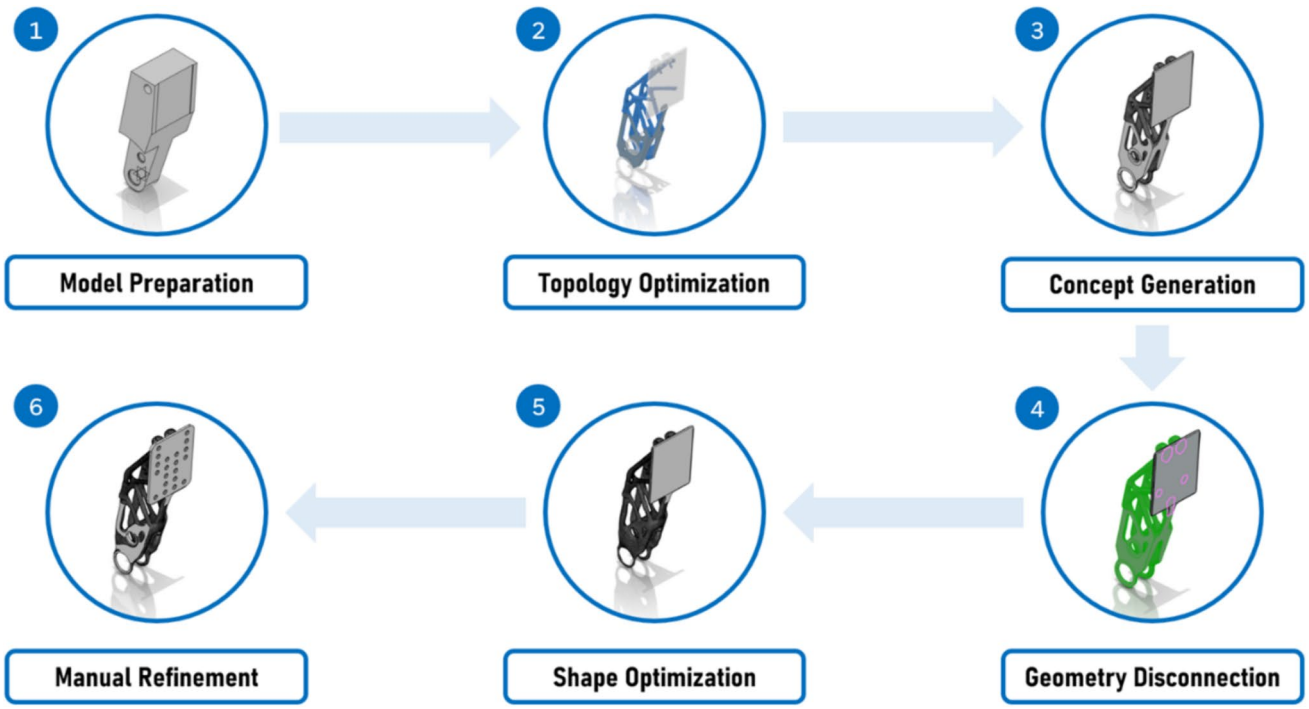

Fig. 10 Schematic of the redesign process using the ABSO workflow

recommended by the tool, which is 6.877 mm, is selected for optimization. Once the optimization is completed, the optimized geometry is generated by selecting the iteration index corresponding to the result with the lowest peak stress value.

4.4.4 Manual refinement

To finalize the redesign process, manual modifications are necessary to ensure that the geometry complies with the limits imposed by the Design Space and guarantees functionality during use. In this case, cuts have been made on the lateral surfaces to ensure assembly onto the structure. Additionally, the Non-Design Space is reconstructed to ensure component functionality, and holes are made on the pad to further lighten the component.

4.5 SOA method redesign

Finally, the redesign is performed using the approach that currently represents the state of the art (Fig. 11).

4.5.1 Design refinement

After the topology optimization is computed, a concept geometry is generated with the Cutting Value set to 57 to achieve a mass similar to the target mass.

Next, the manual redesign process takes place using NURBS surfaces with freeform design tools. During this process, elliptical-section tubular surfaces are drawn to faithfully represent the geometry obtained from the topological optimization. These tubular segments are connected using a merging function, and then the control points are adjusted manually to refine the geometry further. Once the desired surface is obtained, the next step involves creating a solid model by performing a split operation between the surface and a solid body and then adding the non-design areas. Once the geometry formed by NURBS surfaces is obtained, the iterative manual optimization process can begin. Firstly, a physical simulation of the component is conducted, applying loads and constraints as described earlier. Analyzing the simulation results helps identify areas with higher stress concentrations, prompting adjustments to the geometry by manipulating the control points of the NURBS surface to improve the mechanical performance of the part. Subsequently, another physical simulation of the modified geometry is conducted, repeating these two processes iteratively until an optimal stress state is achieved.

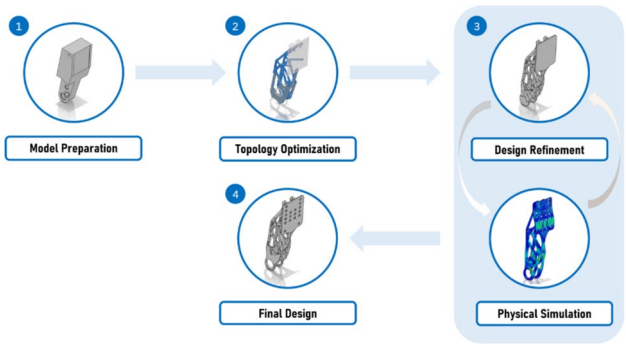

Fig. 11 Schematic of the redesign process using the SOA workflow

4.5.2 Final design

Once the manual redesign process is completed, final adjustments are made to the geometry to ensure that the design space limits are respected, and that assembly and functionality of the component are guaranteed.

5 Discussion

Physical simulations of the obtained geometries, qualitatively displayed in (Fig. 12), are then performed.

The results obtained from the analyses are examined, and the previously selected Key Performance Indicators (KPIs) are compared to evaluate and contrast the outcomes achieved using different workflows (Fig. 13).

5.1 Safety factor

Regarding the safety factor (Fig. 13a), it can be observed that the initial condition has been improved through the redesigns carried out using the ABSO and SOA methods. On the other hand, the redesign performed using the SPO method results in a reduction of the safety factor, although it remains at an acceptable level. It is also important to highlight that the safety factor of the optimized geometries is influenced by the material used for Additive Manufacturing applications, which exhibits inferior mechanical properties compared to the material used for the initial geometry.

5.2 Max displacement

All redesign methods show a significant improvement in maximum displacement values (Fig. 13b) compared to the initial condition, with the new methods achieving results comparable to the SOA method. Specifically, the ABSO method reduces maximum displacement by 51.6%, while the SPO method achieves a reduction of 49.6%.

5.3 Mass

Mass reduction (Fig. 13c) compared to the initial geometry is observed in all configurations, with the ABSO method achieving the most significant reduction at 20.1%,

comparable to the results obtained with the SOA method. The SPO method achieves a reduction of 10.5% relative to the initial geometry.

5.4 Design time

The ABSO method achieves a 52.5% reduction in total design time and an 82.3% decrease in designer working time (Fig. 14a) compared to the SOA method. In contrast, the SPO method results in a 26.1% increase in total design time (Fig. 14a). However, it significantly reduces designer working time by 59.7%.

Figure 14b compares and synthesizes the KPIs' scores for the three design workflows.

6 Conclusions

This paper aims to meet the need for increased integration and automation of DfAM systematic methodologies. The conventional design based on TO requires a time-consuming post-processing stage, and the results are heavily influenced by the designer's experience. The novelty of this work is to define approaches (i.e., ABSO and SPO) which properly exploit numerical tools to streamline the design based on TO, with the aim to produce ready-to-print geometries with minimal user intervention. The approaches make use of commercial software tools, allowing for practical implementation in industrial applications. Two approaches have been developed and compared to the state-of-the-art

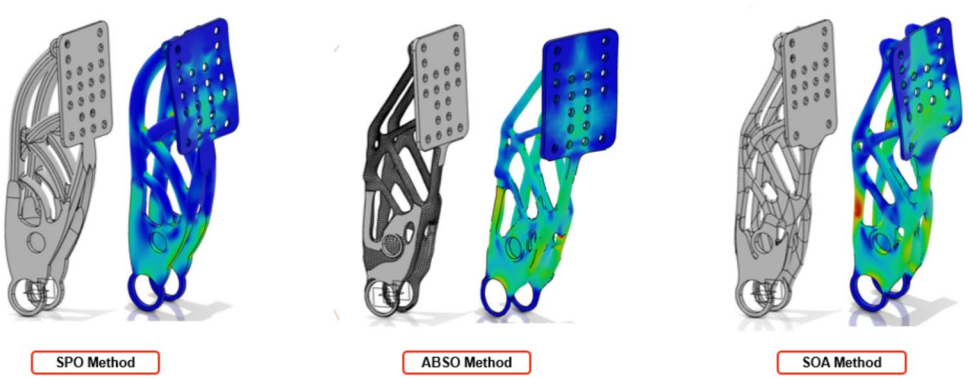

Fig. 12 Geometries obtained from the redesigns, showing the stress distribution for each model

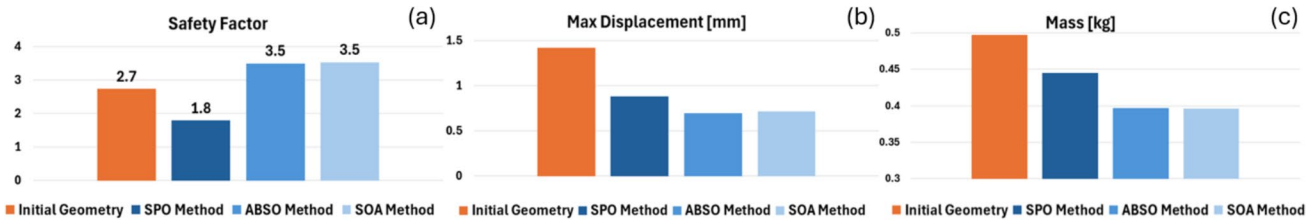

Fig. 13 Mechanical performance key performance indicators

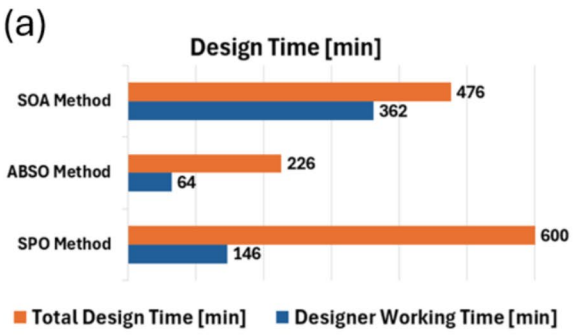

(b)

	Safety Factor	Max Displacement	Mass	Total Design Time	Designer's Working Time
SOA	+	+	++	0	0
ABSO	+	+	++	+	++
SPO	-	+	+	-	+

Fig. 14 KPIs comparing design and working time for human intervention and numerical optimization (**a**) and comparison table of KPIs across different workflows (**b**)

(SOA) workflow with a case study, by selecting KPIs of the mechanical performance and the design process.

The analysis of the results confirms that both the Auto B-Rep Shape Optimization (ABSO) method and the Skeleton-Based Parametric Optimization (SPO) method have successfully met the objectives outlined in this study. These newly developed workflows have enabled the redesign of the MMR Driverless Pedal by leveraging the advantages of additive manufacturing to improve mechanical performance while reducing component weight. Additionally, both approaches eliminate the manual redesign loops inherent in the current state-of-the-art workflow, resulting in a significant reduction in designer working time. Also, compared to related works, both approaches remove the need of design refinement iterations based on FEA, and the ABSO method even removes any manual geometry interpretation modelling step. This outcome highlights the potential for automating the design process, minimizing reliance on designer expertise while achieving optimal results.

Notably, the ABSO method has achieved a design with mechanical performance and weight comparable to those obtained using the SOA method. In contrast, while the SPO method improves upon the initial geometry, its enhancements are less pronounced than those of the ABSO method. In terms of design time, the ABSO method clearly outperforms both methods, demonstrating lower total design time and reduced designer working time. However, despite its lower performance, the SPO method generates the final geometry as a parametric model, allowing for easy modifications and seamless replication. In certain scenarios (e.g., the optimization for conventional manufacturing processes), this flexibility may represent a significant advantage, making the SPO method the preferred choice. It is important to note that using more advanced computational resources, the optimization times of the newly defined workflows could be further reduced. However, manual redesign times in the previously used approach would remain unchanged, further widening the performance gap in favor of the new workflows proposed in this study. Embracing these new approaches could broaden the market acceptance of additive manufacturing, particularly among those who have previously hesitated due to the perceived complexity of the design process.

However, it is important to emphasize that the workflows discussed in this section heavily rely on numerical optimization tools, which play a crucial role in their execution. Currently, these tools have certain limitations that impact their effectiveness in practical applications. In the case of the ABSO method, excellent performance was observed with simpler test geometries, and no significant issues were encountered. However, when dealing with more complex geometries, challenges arose during the Concept Generation phase after calculating the optimal geometry. Reconstructing the optimized geometry proved to be difficult, often due to disconnections made in the geometry during the optimization process. Similarly, the SPO method faces limitations, such as the maximum number of calculation points, which is currently set at 32. Increasing the number of points would undoubtedly improve the optimization result, but it would also extend the computation time. Additionally, manually adjusting parameter values after optimization is another limitation, which could be addressed by automating this process within the software. Moreover, even if the geometry interpretation is not needed, the generation of the Skeleton Wire geometry resulting from topological optimization would greatly benefit from an automated feature within the software that generates sections aligned with the dimensions of the calculated geometry structures. This automation would eliminate the manual intervention required in this study, enhancing the workflow's robustness and replicability.

As computational tools continue to evolve, there will be opportunities to improve both performance and efficiency. With more powerful computing resources, computation times can be significantly reduced, allowing for finer mesh selections and more comprehensive optimization algorithms. Looking ahead, future developments could focus on creating a highly automated Design for Additive Manufacturing process that integrates both design and production phases. This approach would involve multi-objective optimization, considering various process parameters, with the goal of achieving an optimal balance between mechanical performance, material usage, production costs, and build time.

Author contribution Conceptualization, E.D.; Methodology, E.D and L.G.; Validation E.D. and L.G..; Writing—original draft preparation, E.D and L.G.; Writing—review and editing, E.D, L.G., and F.L; supervision, F.L.

All authors read and approved the final manuscript.

Funding Open access funding provided by Università degli Studi di Modena e Reggio Emilia within the CRUI-CARE Agreement.

Declarations

Competing interests The authors declare no competing interests.

References

1. ASTM F2792–12a (2012) Standard terminology for additive manufacturing technologies. ASTM International, West Conshohocken, PA
2. International Organization for Standardization & ASTM International (2021) ISO/ASTM 52900:2021 – Additive manufacturing —General principles — Terminology. ISO. https://www.iso.org/standard/82586.html
3. Gao W, Zhang Y, Ramanujan D, Ramani K, Chen Y, Williams C, Wang C, Shin Y, Zhang S, Zavattieri P (2015) The status, challenges, and future of additive manufacturing in engineering. CAD Comput Aided Zes 66:65–89. https://doi.org/10.1016/j.cad.2015.04.001
4. Tofail SAM, Koumoulos EP, Bandyopadhyay A, Bose S, O'Donoghue L, Charitidis C (2018) Additive manufacturing: scientific and technological challenges, market uptake and opportunities. Mater Today 21(Issue 1):22–37. https://doi.org/10.1016/j.mattod.2017.07.001
5. Ngo TD, Kashani A, Imbalzano G, Nguyen KT, Hui D (2018) Additive manufacturing (3D printing): a review of materials, methods, applications and challenges. Compos Part B 143:172–196. https://doi.org/10.1016/j.compositesb.2018.02.012
6. Pham DT, Gault RS (1998) A comparison of rapid prototyping technologies. Int J Mach Tools Manuf 38(Issues 10–11):1257–1287. https://doi.org/10.1016/S0890-6955(97)00137-5
7. Gu D, Zhang H, Chen H, Zhang H, Xi L (2020) Laser additive manufacturing of high-performance metallic aerospace components. Zhongguo Jiguang/Chin J Lasers 47(5):0500002. https://doi.org/10.3788/CJL202047.0500002
8. Zhu J, Zhou H, Wang C, Zhou L, Yuan S, Zhang W (2021) A review of topology optimization for additive manufacturing: status and challenges. Chin J Aeronaut 34(Issue 1):91–110. https://doi.org/10.1016/j.cja.2020.09.020
9. Blakey-Milner B, Gradl P, Snedden G, Brooks M, Pitot J, Lopez E, Leary M, Berto F, Du Plessis A (2021) Metal additive manufacturing in aerospace: a review. Mater Des 209:110008. https://doi.org/10.1016/j.matdes.2021.110008
10. Gray J, Depcik C (2020) Review of additive manufacturing for internal combustion engine components. SAE Int J Engines 13(5):617–632. https://doi.org/10.4271/03-13-05-0039
11. Sarzynski B, Sniezek L, Grzelak K (2024) Metal Additive Manufacturing (MAM) applications in production of vehicle parts and components—a review. Metals 14:195. https://doi.org/10.3390/met14020195
12. Bendsøe MP, Kikuchi N (1988) Generating optimal topologies in structural design using a homogenization method. Comput Methods Appl Mech Eng 71:197–224. https://doi.org/10.1016/0045-7825(88)90086-2
13. Rozvany GIN, Zhou M, Birker T (1992) Generalized shape optimization without homogenization. Structural Optimization 4:250–252. https://doi.org/10.1007/BF01742754
14. Prathyusha ALR, Raghu Babu G (2022) A review on additive manufacturing and topology optimization process for weight reduction studies in various industrial applications. Mater Today Proc 62:109–117. https://doi.org/10.1016/j.matpr.2022.02.604
15. Ibhadode O, Zhang Z, Sixt J, Nsiempba KM, Orakwe J, Martinez-Marchese A, Ero O, Shahabad SI, Bonakdar A, Toyserkani E (2023) Topology optimization for metal additive manufacturing: current trends, challenges, and future outlook. Virtual Phys Prototyp. https://doi.org/10.1080/17452759.2023.2181192
16. Tang Y, Zhao YF (2016) A survey of the design methods for additive manufacturing to improve functional performance. Rapid Prototyping J 22(3):569–590. https://doi.org/10.1108/RPJ-01-2015-0011
17. Bourell DL, Leu MC, Rosen DW (2009) Roadmap for additive manufacturing identifying the future of freeform processing. University of Texas for Freeform Fabrication Advanced Manufacturing Center, Austin
18. Kumke M, Watschke H, Vietor T (2016) A new methodological framework for design for additive manufacturing. Virtual Phys Prototyp 11:3–19. https://doi.org/10.1080/17452759.2016.1139377
19. Pradel P, Zhu Z, Bibb R, Moultrie J (2018) A framework for mapping design for additive manufacturing knowledge for industrial and product design. J Eng Des 29(6):291–326. https://doi.org/10.1080/09544828.2018.1483011
20. Wiberg A, Persson J, Ölvander J (2019) Design for additive manufacturing – a review of available design methods and software. Rapid Prototyp J 25(6):1080–1094. https://doi.org/10.1108/RPJ-10-2018-0262
21. Vaneker T, Bernard A, Moroni G, Gibson I, Zhang Y (2020) Design for additive manufacturing: framework and methodology. CIRP Ann 69(2):578–599. https://doi.org/10.1016/j.cirp.2020.05.006
22. Sotomayor N, Caiazzo F, Alfieri V (2021) Enhancing design for additive manufacturing workflow: optimization, design and simulation tools. Appl Sci 11:6628. https://doi.org/10.3390/app11146628
23. Gebisa A, Lemu H (2017) A case study on topology optimized design for additive manufacturing. In: IOP Conference Series: Materials Science and Engineering, vol. 276, no. 1, p 012026. https://doi.org/10.1088/1757-899X/276/1/012026
24. Orme M, Madera I, Gschweitl M, Ferrari M (2018) Topology optimization for additive manufacturing as an enabler for light weight flight hardware. Des 2(4):51. https://doi.org/10.3390/designs2040051
25. Reddy SN, Maranan V, Simpson TW, Palmer T, Dickman CJ (2016) Application of topology optimization and design for additive manufacturing guidelines on an automotive component. Proceedings of the ASME Design Engineering Technical Conference, 2A-2016. https://doi.org/10.1115/DETC2016-59719
26. Walton D, Moztarzadeh H (2017) Design and development of an additive manufactured component by topology optimization. Procedia CIRP 60:205–210. https://doi.org/10.1016/j.procir.2017.03.027
27. Mantovani S, Barbieri S, Giacopini M, Croce A, Sola A, Bassoli E (2021) Synergy between topology optimization and additive manufacturing in the automotive field. Proceedings of the Institution of Mechanical Engineers, Part B: Journal of Engineering Manufacture 235(3):555–567. https://doi.org/10.1177/0954405420949209
28. Barbieri L, Muzzupappa M (2022) Performance-driven engineering design approaches based on generative design and topology optimization tools: a comparative study. Appl Sci 12:2106. https://doi.org/10.3390/app12042106
29. Ugemuge M, Das S (2020) Topology optimisation of brake caliper. SAE Technical Paper 2020–01–1620. https://doi.org/10.4271/2020-01-1620
30. Tyflopoulos E, Lien M, Steinert M (2021) Optimization of brake calipers using topology optimization for additive manufacturing. Appl Sci 11:1437. https://doi.org/10.3390/app11041437
31. Booth JW, Alperovich J, Chawla P, Ma J, Reid TN, Ramani K (2017) The design for additive manufacturing worksheet. J Mech Des 139(10):100904. https://doi.org/10.1115/1.4037251
32. Alfaify A, Saleh M, Abdullah FM, Al-Ahmari AM (2020) Design for additive manufacturing: a systematic review. Sustainability (Switzerland) 12(19):7936. https://doi.org/10.3390/su12197936

33. Egan PF (2023) Design for additive manufacturing: recent innovations and future directions. Designs 7:83. https://doi.org/10.3390/designs7040083
34. Schaechtl P, Goetz S, Schleich B, Wartzack S (2023) Knowledge-driven design for additive manufacturing: a framework for design adaptation. Proc Des Soc 3:2405–2414. https://doi.org/10.1017/pds.2023.241
35. Dalpadulo E, Pini F, Leali F (2022) Optimization of an engine piston through CAD platforms and additive manufacturing based systematic product redesign. In: Rizzi C, Campana F, Bici M, Gherardini F, Ingrassia T, Cicconi P (eds) ADM 2021. LNME. Springer, Cham, pp 486–493. https://doi.org/10.1007/978-3-030-91234-5_49
36. Dalpadulo E, Pini F, Leali F (2024) Powder bed fusion integrated product and process design for additive manufacturing: a systematic approach driven by simulation. Int J Adv Manuf Technol 130:5425–5440. https://doi.org/10.1007/s00170-024-13042-8
37. Holub P, Gulan L, Korec A, Chovanˇcíková V, Nagy M, Nagy M (2023) Application of advanced design methods of "Design for Additive Manufacturing" (DfAM) to the process of development of components for mobile machines. Appl Sci 13:12532. https://doi.org/10.3390/app132212532
38. Fuchs D, Bartz R, Kuschmitz S, Vietor T (2022) Necessary advances in computer-aided design to leverage on additive manufacturing design freedom. Int J Interact Des Manuf. https://doi.org/10.1007/s12008-022-00888-z
39. Xiao Z, Yang Y, Wang D, Song C, Bai Y (2018) Structural optimization design for antenna bracket manufactured by selective laser melting. Rapid Prototyping J 24(3):539–547. https://doi.org/10.1108/RPJ-05-2017-0084
40. Tyflopoulos E, Steinert M (2020) Topology and parametric optimization-based design processes for lightweight structures. Appl Sci 10(13):4496. https://doi.org/10.3390/app10134496
41. Biedermann M, Beutler P, Meboldt M (2021) Automated design of additive manufactured flow components with consideration of overhang constraint. Addit Manuf 46:102119. https://doi.org/10.1016/j.addma.2021.102119
42. Amroune A. Cuillière JC, François V (2022) Automated lofting-based reconstruction of CAD models from 3D topology optimization results, computer-aided design 145:103183. https://doi.org/10.1016/j.cad.2021.103183
43. Mayer J, Völkl H and Wartzack S (2022) Feature-based reconstruction of nonbeam-like topology optimization design proposals in boundary-representation, In Proceedings of the 33rd Symposium Design for X, DFX 2022. The Design Society. https://doi.org/10.35199/dfx2022.21
44. Mayer J, Wartzack S (2023) Computational geometry reconstruction from 3D topology optimization results: a new parametric approach by the medial axis. Comp-Aided Des Appl 20(5):960–975. https://doi.org/10.14733/cadaps.2023.960-975
45. Sedlacek F, Kalina T, Stepanek M (2023) Optimization of components with topology optimization for direct additive manufacturing by DLMS. Materials 16:5422. https://doi.org/10.3390/ma16155422
46. Ravichandran K, Masoudi N, Fadel GM, Wiecek MM (2019) Parametric optimization for structural design problems. Proceedings of the ASME 2019 International Design Engineering Technical Conferences and Computers and Information in Engineering Conference, Volume 2B: 45th Design Automation Conference, Anaheim, California, USA, August 18–21, 2019. ASME. https://doi.org/10.1115/DETC2019-97860
47. Le C, Bruns T, Tortorelli D (2011) A gradient-based, parameter-free approach to shape optimization. Comput Methods Appl Mech Eng 200(9–12):985–996. https://doi.org/10.1016/j.cma.2010.10.004
48. Reiher T, Vogelsang S, Koch R (2017) Computer integration for geometry generation for product optimisation with additive manufacturing, in Solid Freeform Fabrication 2017: Proceedings of the 28th Annual International Solid Freeform Fabrication Symposium - An Additive Manufacturing Conference, SFF 2017, The University of Texas at Austin, pp 903–921. https://hdl.handle.net/2152/89890. Accessed 3 June 2025
49. Dalpadulo E, Pini F, Leali F (2024) Numerically driven geometrical modeling and refinement approaches to streamline the design of topology optimized parts: a comparative study. Proceedings of the ASME 2024 International Mechanical Engineering Congress and Exposition. Volume 1: Acoustics, Vibration, and Phononics; Advanced Design and Information Technologies. Portland, Oregon, USA. November 17–21, 2024. ASME. https://doi.org/10.1115/IMECE2024-145490